A diffusion-driven device for a high-resolution dose-response profiling of combination chemotherapy

Alexander Ganser,[†,#,%] Günter Roth,[¶,#,£] Joost C. van Galen,[$] Janneke Hilderink,[†] Joost J. G. Wammes,[†] Ingo Müller,[§] Frank N. van Leeuwen,[$] Karl-Heinz Wiesmüller,[‡] Roland Brock[¶,†,*]

[†]Department of Biochemistry, Nijmegen Centre for Molecular Life Sciences, Radboud University Nijmegen Medical Centre, Nijmegen, The Netherlands

[$]Department of Pediatrics, Laboratory of Pediatric Oncology, Radboud University Nijmegen Medical Centre, Nijmegen, The Netherlands

[§]Department of General Pediatrics, Hematology and Oncology, University Children's Hospital, Tübingen, Germany

[¶]Department of Molecular Biology, Interfaculty Institute for Cell Biology, Eberhard Karls University Tübingen, Tübingen, Germany

[‡]EMC microcollections GmbH, Tübingen, Germany

[%]present address: EMC microcollections GmbH, Tübingen, Germany

[£]present address: Department of Microsystems Engineering, Institute of Microsystem Technology (IMTEK), University of Freiburg, Freiburg

*to whom correspondence should be addressed: Department of Biochemistry, Nijmegen Centre for Molecular Life Sciences, Radboud University Nijmegen Medical Centre, PO Box 9101, 6500 HB Nijmegen, The Netherlands, r.brock@ncmls.ru.nl

#These authors contributed equally to this work

Supporting Information

- calibration of fluorophore concentrations and fluorescence image analysis
- solvent independence of concentration gradients
- time-weighted average
- combination index according to Chou
- Supporting Information Figures S-1 – S-8

Calibration of fluorophore concentrations and fluorescence image analysis. For initial experiments in which the formation of concentration gradients was validated, a robust protocol for the determination of fluorophore concentrations was needed. To convert fluorescence intensities from fluorophores within the gel matrix of the diffusion device into concentrations, calibration curves were generated using solutions of fluorophores of known concentrations. Rhodamine B and fluorescein either alone or mixed were diluted into water, PBS, agarose and gelatin using different concentrations of gelating compound (agarose 1.5 % (w/v) and 2 % (w/v), gelatin 5 % (w/v) and 10 % (w/v)). The solutions were pipetted into wells of 96-well plates and image acquisition was carried out under the same conditions as measurements with the diffusion device. For all images, nine identically positioned regions-of-interest (ROI) were selected and average pixel intensities were calculated. In order to account for different image acquisition times for solutions of high and low concentrations the grey value of every concentration was calculated back to 1 millisecond acquisition time. In a first step, the concentration dependence on fluorophore concentration was investigated in detail (Figure S-2). Especially at higher fluorophore concentrations, self quenching and energy transfer from fluorescein to rhodamine led to deviations from a linear concentration dependence. In comparison to agarose, gelatin affected the fluorescence intensities in dependence of the fluorophores (fluorescence intensity increased for rhodamine and decreased for fluorescein). Once this information had been recorded, on later days, measurement of only four concentrations was sufficient for determination of a correction factor representing the ratios of fluorescence intensities at the different measurement days. With this correction factor, fluorescence of the gradients could be related to the corresponding fluorophore concentration. In this way, it was possible to correct for day-to-day variations in excitation intensity.

For doxorubicin a calibration curve was generated by measuring the fluorescence intensity of different doxorubicin concentrations in medium containing 10 % FCS in a 96-well plate, using a confocal laser scanning microscope for detection. The fluorescence of doxorubicin had a sigmoidal dependence on the concentration. Gradients in the diffusion device were averaged over three line profiles of fluorescence extracted from a tile scan of the whole assay area.

Solvent independence of concentration gradients. Drug candidates are frequently diluted from DMF or DMSO stock solutions. Given the fact that in cellular assays solvent concentrations should not exceed 1 % (v/v) and considering the 1:10 dilution of substances from the substance application slot to the start of the gradient in the assay chamber, rhodamine was diluted either in PBS or PBS with DMF and DMSO (10 % (v/v)) and the concentration profiles were recorded at different times of gradient formation. The presence of organic solvent was without effect on the formation of concentration gradients (Figure S-4).

Time-weighted average. To consider the temporal evolution of the diffusion-generated concentration gradients we calculated a time-weighted average concentration which we used for the determination of dose-response functions. In this procedure a concentration gradient was calculated for each hour and the effective concentration at each location calculated according to eq. S-1.

$$c_{effective} = \frac{\sum_{t=1}^{t_{\max}} \left(t_{\max} - t + 1\right) \times c_t}{\sum_{t=1}^{t_{\max}} \left(t_{\max} - t + 1\right)} \quad \text{(eq. S-1)}$$

Combination Index according to Chou. The calculation of the Combination Index (CI) is based on the dose-response curves for every single drug and the combination of the drugs. A constant mixing ratio of the drugs for every combination facilitates the calculation of CI values. Dose response functions for the individual drugs and the combination are plotted with log values of the

concentration and the related effect grade (from 0 to 1) (Figure S-7). The intersections with the x-axis, corresponding to the EC_{50} value, and the slopes of the straight lines must be determined. With these parameters combination indices can be calculated according to equations S-3 to S-8[1]:

$$D_{(effect)1} = EC_{50\ substance\ 1} \times (effect/1\text{-}effect)^{(1/slope\ substance\ 1)} \quad \text{(eq. S-2)}$$

$$D_{(effect)2} = EC_{50\ substance\ 2} \times (effect/1\text{-}effect)^{(1/slope\ substance\ 2)} \quad \text{(eq. S-3)}$$

$$D_{(effect)combination} = EC_{50\ combination} \times (effect/1\text{-}effect)^{(1/slope\ combination)} \quad \text{(eq. S-4)}$$

$$D_{1\ combination} = EC_{50\ combination} \times (r)/(r+1) \quad \text{(eq. S-5)}$$

$$D_{2\ combination} = EC_{50\ combination} \times 1/(r+1) \quad \text{(eq. S-6)}$$

$$CI_{\ mutually\ exclusive} = D_{1\ combination} / D_{(effect)1} + D_{2\ combination} / D_{(effect)2} \quad \text{(eq. S-7)}$$

$$CI_{\ mutually\ non\text{-}exclusive} = D_{1\ combination}/ D_{(effect)1} + D_{2\ combination}/ D_{(effect)2} + D_{1\ combination} \times D_{2\ combination} / (D_{(effect)1} \times D_{(effect)2}) \quad \text{(eq. S-8)}$$

Effect relates to the fraction of target affected, in our case the fraction of dead cells. $D_{(effect)x}$ (with x equals to substance 1, 2, or the combination) denotes the concentration of substance 1, 2 or the combination that is needed to cause a specific effect (0-1). $D_{x\ combination}$ with x equals to substance 1, or 2, is the concentration of substance 1 or 2 in the combination which is needed to reach a specific effect, r is the concentration ratio of substances 1 and 2 in the combination, CI denotes the combination index.

In our case CI values were determined along the diagonal of the diffusion device that originates from where both application slots meet. With identical diffusion coefficients of both substances, in this case, along the diagonal effects for constant ratios r of both substances were obtained. The ratio corresponded to the ratio of concentrations in the application slots.

Chou et al. suggested a classification of CI-indices as follows: 0.9 – 1.1 is additive; 1.1 – 1.2 is slightly antagonistic, 1.2 – 1.45 is moderately antagonistic; 1.45 – 3.3 is antagonistic, 3.3 – 10 is strongly antagonistic and > 10 is very strongly antagonistic. Furthermore, 0.85 – 0.9 is slightly synergistic; 0.7 – 0.85 is moderately synergistic; 0.3 – 0.7 is synergistic; 0.1 – 0.3 is strongly synergistic and < 0.1 is very strongly synergistic. Examples for CI-diagrams are shown in Figure 4 and Figure S-8.

SUPPORTING INFORMATION – FIGURES

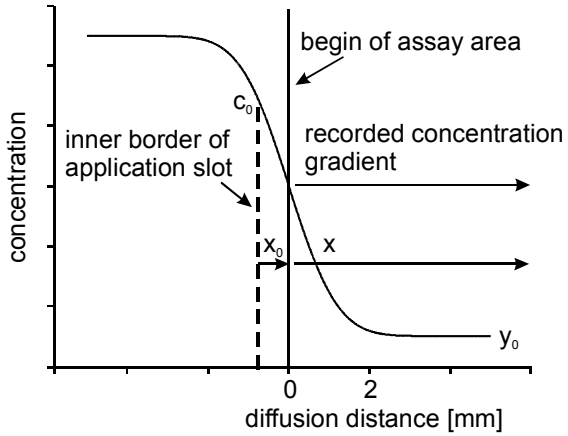

Figure S-1. Schematic depiction of the diffusion device superimposed on the error function. The error function is employed to describe diffusion from an unlimited source. C_0 is the concentration underneath the application slot that is related to the concentration inside the application slot by a factor of 7 (1.4 times the concentration of a ten-fold dilution of the concentration in the application slot). The concentration at the edge of the assay area at x_0 is related to the concentration in the application slot by a factor of ten. Y_0 is an offset that, in the case of recording of concentration gradients for fluorescent substances, corresponds to background fluorescence.

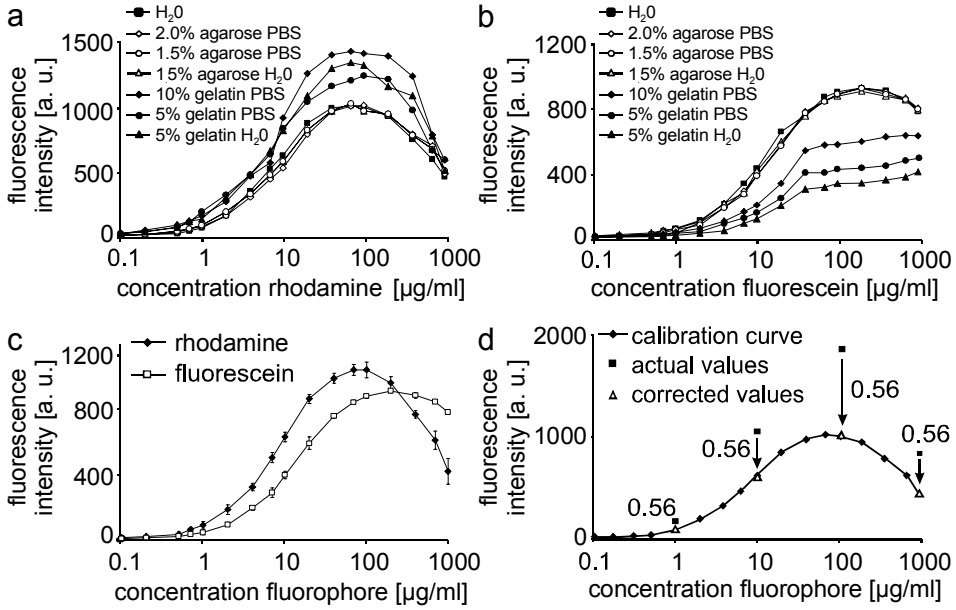

Figure S-2. Calibration of the diffusion device. (a, b) Fluorescence intensity over concentration for (a) rhodamine B and (b) fluorescein in water, and agarose and gelatin matrices of different concentrations prepared either with water or PBS. (c) Fluorescence intensity versus concentration for fluorescein and rhodamine. Shown are averages for water, and 1.5 % and 2 % agarose prepared in PBS and water. (d) Calibration curve for rhodamine B with actual and corrected values for four calibration solutions. The numbers next to the arrows correspond to the relative intensities of the four concentrations to the respective intensities measured at a reference day, when all concentrations were measured. With the average of these four values, all intensities acquired for rhodamine from a diffusion device could be calculated back to reference intensities.

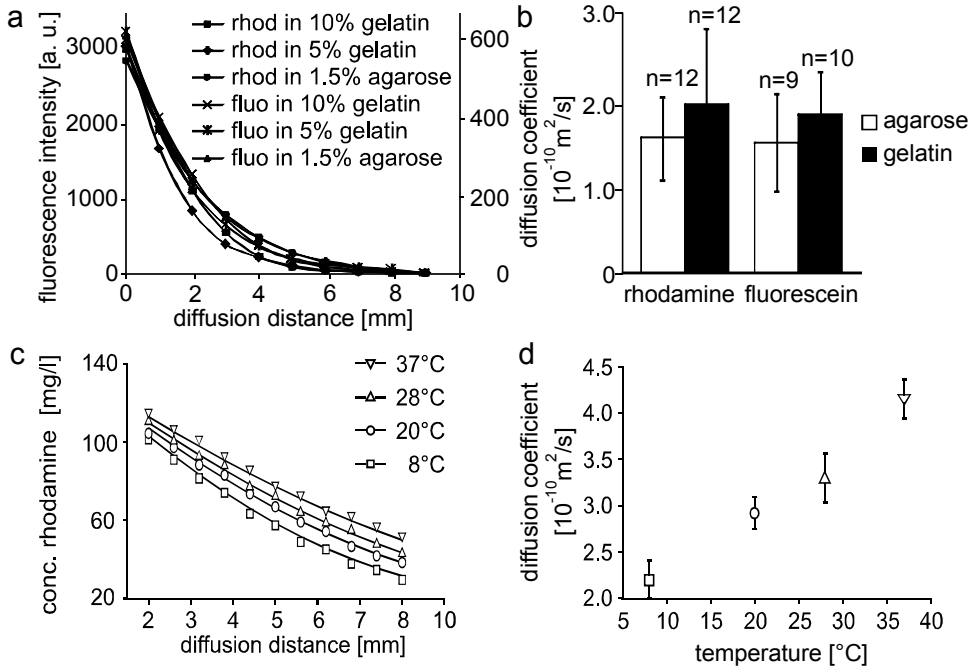

Figure S-3. Diffusion of fluorophores. (a) Concentration profiles of fluorescein and rhodamine B in gelatin (5 and 10% w/v) and agarose (1.5% w/v) recorded after 7 h of diffusion. All curves can be described by an error function assuming a constant source boundary condition of diffusion. Fluorescence intensities for rhodamine B are given on the left y-axis, intensities for fluorescein on the right y-axis. (b) Diffusion coefficients for fluorescein and rhodamine in agarose (1.5 % w/v) and gelatin (average of values determined for 5 and 10 % gelatin. For 1.5 % agarose, diffusion constants were $2.18 \pm 0.77 \times 10^{-10}$ m^2s^{-1} for rhodamine B and $2.23 \pm 0.61 \times 10^{-10}$ m^2s^{-1} for fluorescein. The total number of independent measurements is given on top of each bar. Error bars correspond to standard deviations of the mean. (c, d) Temperature dependence of diffusion. (c) Concentration profiles of rhodamine obtained for diffusion at different temperatures. The concentration of fluorescein in the application slot was 1 g/l and the diffusion time was 36 h. (d) Diffusion coefficients derived from the data in (c) using a model of constant source boundary condition (C). The error bars correspond to the 95 % confidence interval of the fit.

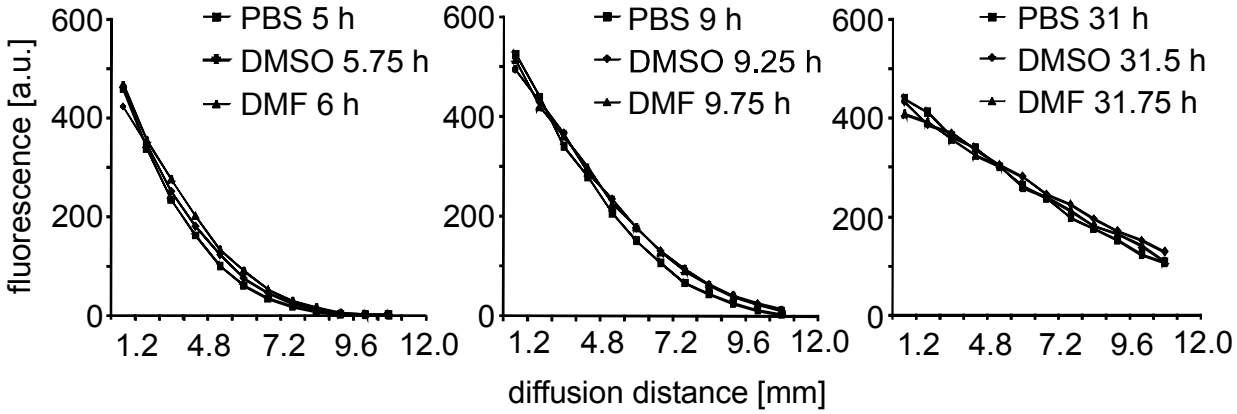

Figure S-4. Influence of organic solvents on gradient formation. Rhodamine was diluted to a concentration of 100 µg/ml either in PBS or in PBS containing DMSO or DMF (10 % (v/v)). At the indicated times, fluorescence profiles were recorded.

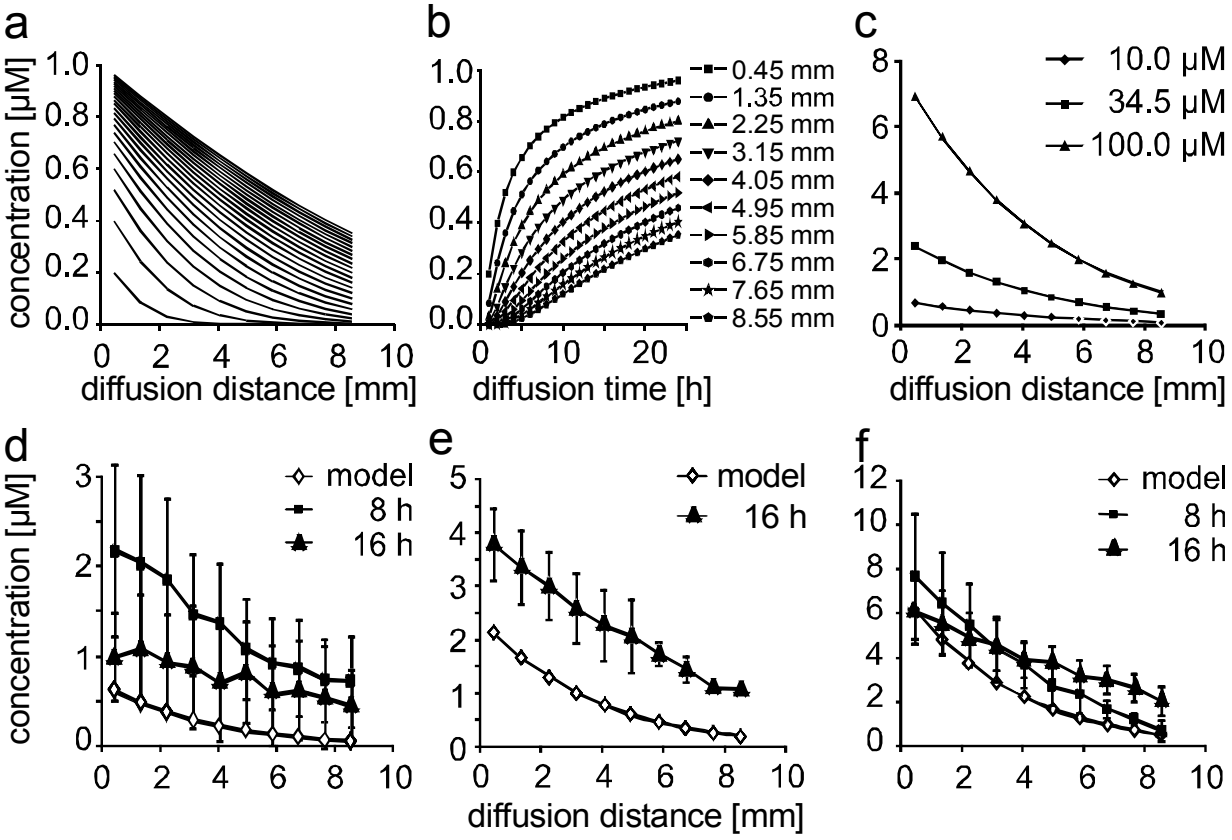

Figure S-5: Calculation of effective concentrations using a time-weighted average. (a) Time dependence of concentration gradients simulated by assuming a diffusion model following Fick's laws with an infinite diffusion source and a diffusion coefficient of 6.14 x 10^{-10} m^2s^1. (b) Temporal evolution of concentrations at different locations along the test area over time (simulation parameters: 10 µM start concentration, 24 h diffusion time, diffusion coefficient 6.14 x $10^{-10}m^2s^{-1}$) (c) Averaged concentration profiles for doxorubicin, etoposide and clofarabine with the starting concentrations which were used in the following experiments (34.5 µM doxorubicin, 10 µM clofarabine and 100 µM for etoposide). The curves represent a concentration calculated by time-weighted averaging over 0 to 24 h. For clofarabine and etoposide the diffusion constant of doxorubicine that was determined experimentally for doxorubicin was applied. (d-f) Comparison of weighted averages and experimental data for two

specific time points at start concentrations of (d) 10 µM, (e) 34.5 µM, and (f) 100 µM. The experimental data was obtained for doxorubicine at 8 and 16 h after initiation of diffusion. The weighted averages were calculated using the diffusion constant of doxorubicine and a dilution factor of ten as described. At a concentration of 34.5 µM, concentration profiles were only acquired after 16 h. It should be noted that the concentrations in the model are lower than the ones for a specific time point, due to the calculation of time-weighted averages.

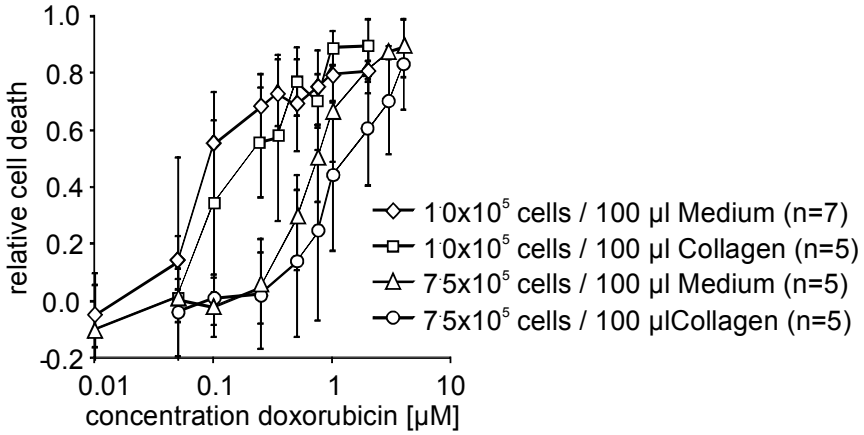

Figure S-6. Dependence of doxorubicin-induced cytotoxicity on cell density and embedding of cells into collagen. The experiments were carried out with MOLT-4 cells in microtiter plates. EC_{50} values were: 72 nM for 50,000 cells in 50 µl medium; 190 nM for 50,000 cells in 50 µl collagen matrix; 0.76 µM for 375,000 cells in 50 µl medium and 1.56 µM for 375,000 cells in 50 µl collagen matrix. The plots are the means of n experiments. EC_{50} values were determined for the resulting average curves.

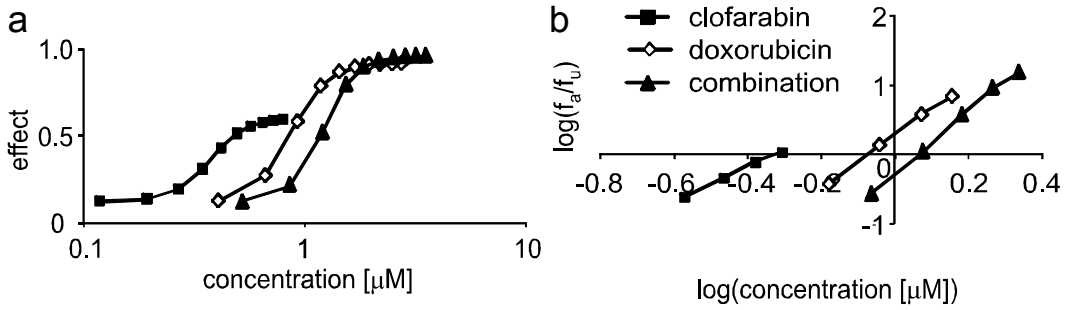

Figure S-7. (a) Dose-response curves for single agents and the drug combination. The dose-response curve for the drug combination was extracted along the diagonal of the assay area, therefore corresponding to a constant concentration ratio of both substances that corresponded to the ratio of the concentrations of both substances in the application slots. (b) "Median-effect" plot for the dose response profiles shown in (a). f_a relates to the "fraction affected", which for the testing of cytotoxic drugs is the fraction of dead cells, and f_u to the fraction unaffected, which is the fraction of viable cells corresponding to 1-f_a. The intersection of the graphs with the x-axis corresponds to the EC_{50} values.

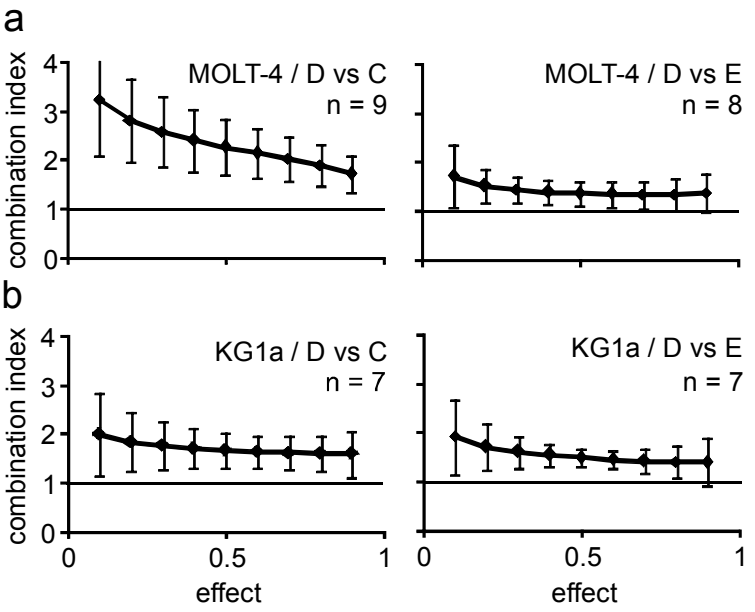

Figure S-8. Comparison of CI profiles for (a) MOLT-4 and (b) KG1a cells. Error bars represent the standard deviations of the means. The number of independent experiments from which the averages were calculated are shown in each graph.

Supporting Information Reference List

1. Chou, T. C.; Talalay, P. *Adv.Enzyme Regul.* **1984,** *22*, 27-55.